Available online at www.sciencedirect.com
ScienceDirect
Journal of Molecular Graphics and Modelling 25 (2006) 196–207
Journal of Molecular Graphics and Modelling
www.elsevier.com/locate/JMGM

Homology modeling of human sialidase enzymes NEU1, NEU3 and NEU4 based on the crystal structure of NEU2: Hints for the design of selective NEU3 inhibitors

Sadagopan Magesh [a,*], Tohru Suzuki [b], Taeko Miyagi [c], Hideharu Ishida [a], Makoto Kiso [a,d,*]

[a] Department of Applied Bioorganic Chemistry, Gifu University, Gifu 501-1193, Japan
[b] Life Science Research Center, Gifu University, Gifu 501-1193, Japan
[c] Division of Biochemistry, Research Institute, Miyagi Prefectural Cancer Center, Natori, Miyagi 981-1293, Japan
[d] CREST, Japan Science and Technology Corporation (JST), Tokyo, Japan

Received 13 October 2005; received in revised form 15 December 2005; accepted 16 December 2005
Available online 19 January 2006

Abstract

Four types of human sialidases have been cloned and characterized at the molecular level. They are classified according to their major intracellular location as intralysomal (NEU1), cytosolic (NEU2), plasma membrane (NEU3) and lysosomal or mitochondrial membrane (NEU4) associated sialidases. These human isoforms are distinct from each other in their enzymatic properties as well as their substrate specificity. Altered expression of sialidases has been correlated with malignant transformation of cells and different sialidases have been known to behave differently during carcinogenesis. Particularly, increased expression of NEU3 has been implicated in the survival of various cancer cells and also in the development of insulin resistance. In the present study, we have modeled three-dimensional structures of NEU1, NEU3 and NEU4 based on the crystal structure of NEU2 using the homology modeling program MODELER. The best model in each enzyme case was chosen on the basis of various standard protein analysis programs. Predicted structures and the experimental protein–ligand complex of NEU2 were compared to identify similarities and differences among the active sites. The molecular electrostatic potential (MEP) was calculated for the predicted models to identify the differences in charge distribution around the active site and its vicinity. The primary objective of the present work is to identify the structural differences between the different isoforms of human sialidases, namely NEU1, NEU2, NEU3 and NEU4, thus providing a better insight into the differences in the active sites of these enzymes. This can in turn guide us in the better understanding and rationale of the differential substrate recognition and activity, thereby aiding in the structure-based design of selective NEU3 inhibitors.

Keywords: Homology modeling; Comparative modeling; Sialidase (neuraminidase); Structure-based inhibitor design; Molecular electrostatic potential (MEP); Active site modeling

1. Introduction

Sialidases (E.C.3.2.1.18) also known as neuraminidases belong to a group of glycohydrolytic enzymes, which remove sialic acid residues from a variety of sialoglycoconjugates. They are widely distributed among the different classes of organisms such as viruses, bacteria, protozoa and vertebrates [1]. Sialidases are thought to be involved in various biological processes like infection, proliferation, differentiation, catabolism, signal transduction, antigenic properties and inter–intra cell interactions [2].

Several mammalian sialidases have been cloned and characterized at the molecular level. In humans, four types of sialidases are known and have been classified based on their subcellular localization as intra lysosomal (NEU1) [3,4], cytosolic (NEU2) [5,6], plasma membrane (NEU3) [7,8] and lysosomal or mitochondrial membrane (NEU4) [9]. A comparison of human sialidases with respect to their location, substrate specificity, function and the changes they undergo in cancer cells has been described elsewhere in literature [10]. In addition to subcellular localization, these sialidases also differ

* Corresponding authors. Tel.: +81 58 293 2916/2918; fax: +81 58 293 2840.
E-mail addresses: sadagopan_magesh@rediffmail.com (S. Magesh), kiso@cc.gifu-u.ac.jp (M. Kiso).

1093-3263/$ – see front matter © 2005 Elsevier Inc. All rights reserved.
doi:10.1016/j.jmgm.2005.12.006

in substrate preferences, pH required for optimum activity and also in immunological properties. Despite their different locations and substrate specificities, all human sialidases have highly conserved active site residues, the F/YRIV/P motif in the N-terminal part and the Asp boxes (consensus S/TXD(X)GXTW/F present as three to five repeat in the protein) similar to their viral and bacterial counter parts [11]. These results indicate a monophyletic origin of the sialidases and thus giving the basis for molecular modeling studies to elucidate the structure–function relationships between the family members. The comparative biochemistry and molecular biology of human sialidases has been reviewed excellently elsewhere [2].

Lysosomal sialidase (NEU1) possesses narrow substrate specificity for oligosaccharides, glycopeptides and a synthetic substrate 4MU-Neu5Ac (4-methylumbelliferyl-*N*-acetylneuraminic acid) [12] and is involved in lysosomal catabolism of sialoglycoconjugates by collaborating with lysosomal proteases or endoglycosidases [13]. Lysosomal storage diseases like sialidosis and galactosialidosis caused by NEU1 deficiency, interferes with the pathways for degradation of sialylated glycoconjugates [3,14]. In addition to this NEU1 has been proposed to be involved in cellular signaling during immune responses as well as monocytes differentiation [15,16]. Cytosolic sialidase (NEU2) is active against oligosaccharides, glycopeptides and gangliosides [17]. In mammals, it has been implicated in myotube formation [18]. The exact mechanism of myoblast differentiation through its natural substrate remains obscure but it is claimed to decrease the GM3 ganglioside content, associated with the cytoskeleton [19]. Plasma membrane sialidase (NEU3) hydroyzes gangliosides specifically (except GM1 and GM2) in presence of non-ionic surfactant (Triton X-100) [8,20,21]. Since gangliosides are abundant on the plasma membrane and are known modulators of several surface events like cell differentiation, cell proliferation and signal transduction, NEU3 is expected to be involved in cell surface functions by modulating gangliosides [22]. NEU3 involvement in neural differentiation has also been described in literature [23]. Lysosomal or mitochondrial membrane sialidase (NEU4) has broad specificity, active against all major sialoglycoconjugates and has been implicated in the catabolism of glycolipids [11,24]. A recent report reveals the possibility of NEU4 being involved in apoptosis pathway at the mitochondrial level by regulating ganglioside GD3 [24]. Further functions of NEU4 are yet to be explored.

Further, there is also some correlation between sialidase expression and the alteration in sialyation levels during malignant transformation of cells [10,22]. In murine, overexpression of lysosomal sialidase in cancer cells showed suppression of metastasis and tumor progression as well as increased sensitivity to apoptosis. Cytosolic sialidase overexpression in melanoma and colonadenocarcinoma cells of mouse has been inversely correlated with their invasiveness and metastatic potential, which is associated with a decrease in sialyl Lewis X and GM3 as well. Although it has been reported that NEU3 is not associated with metastatic potential and invasiveness, certain human cancer cells showed increased expression of NEU3 [25]. This increased expression resulted in inhibition of apoptosis accompanied by increased expression of Bcl2, followed by decreased expression of caspase. Inhibitory role of NEU3 in apoptosis is proposed to be mediated by accumulation of a possible sialidase product lactosyl ceramide (Lac-Cer), which induces Bcl2 expression or by rapid degradation of GD3 [25]. In addition, NEU3 mediated gangliosides depletion results in the activation of integrin-induced kinase/Akt, followed by deactivation of caspase-9 in SCCl2 cells [26]. A recent review discusses distinct aspects of NEU3 inhibition and its relevance in the cure of cancer [22]. NEU3 is also found to be involved in insulin signaling in two ways [27]. First is the negative regulation of insulin signaling by associating with the Grb2 protein and second is the suppression of insulin receptor (IR) phosphorylation through the modulation of gangliosides. Taken together, these anomalous functions of NEU3 are different from the possible regulatory functions of other human sialidases. So selective NEU3 inhibition may be a useful approach in cancer and diabetes therapy or in any case would be a valuable tool for exploring differential functions of human sialidases. The sialic acid transition-state analogue, DANA (2-deoxy-2,3-dehydro-*N*-acetylneuraminic acid) is available as a weak inhibitor of sialidase enzymes, but it is not selective for NEU3. Structure-based approach in this regard may provide hints on how to exploit the non-selective inhibitor substituents that extend out of the active site pocket or 'de novo design' for isoform-selective inhibitor design. Structure homology and sequence alignment methods have been very useful in structure-based design approaches and can tackle the challenge of selectivity. Moreover, the success story of the structure-based drug design of viral sialidase inhibitors for flu fever through computational analysis giving the impetus for our efforts in this subject.

In the present study, we report homology models of NEU1, NEU3 and NEU4 using the crystal structure of NEU2. Using homology models, we have studied active site and its vicinity of human sialidases, which can be exploited for the design of selective NEU3 inhibitors.

2. Methods

All computations and simulations were carried out on an Intel P4 based Microsoft windows 2000 workstation using Discovery Studio Modeling 1.1 Package (Accelrys) [28].

2.1. Template search

The amino acid sequences of NEU1 (accession no. Q99519, entry name: NEUR1_HUMAN), NEU3 (accession no. Q9UQ49, entry name: NEUR3_HUMAN) and NEU4 (accession no. Q8WWR8, entry name: NEUR4_HUMAN) were obtained from Swiss-Prot database [29]. The Gapped-BLAST [30] through NCBI was used to identify homologous structures by searching the structural database of protein sequences in the protein data bank (PDB) [31] using *DS protein similarity* search module. The crystal structure of human NEU2 (PDB code: 1VCU, Chain B) was selected as a template for homology modeling of NEU1, NEU3 and NEU4 [32].

2.2. Sequence/template alignment

The amino acid sequences of NEU1, NEU3 and NEU4 were aligned with sequence of NEU2 extracted from its crystal structure, using the Align123 of *DS protein families* module, which is shown in Fig. 1. The Blosum scoring matrix was selected with a gap penalty of 10 and a gap extension penalty of 0.05. Align123 is a multiple sequence alignment method based on the CLUSTAL W program [33], which aligns multiple sequences using a progressive pairwise alignment algorithm. Alignments were checked for deletions and insertions in structurally conserved regions and finally fine-tuned manually. The sequences of NEU1, NEU3 and NEU4 were aligned to NEU2 individually based upon the multiple alignments obtained above and then each case was visually edited for the alignments of conserved and chemically similar residues.

2.3. Model generation

Homology models of NEU1, NEU3 and NEU4 were constructed using the *DS MODELER* module (default parameters), based upon the individual sequence/template alignments. MODELER is a well-known comparative modeling methodology, which generates a refined 3D homology

```
HsNEU1   1   MTGERPSTALPDRRWGPRILGFWGGCRVWVFAAIFLLLSLAASWSKAENDFGLVQPLVTMEQLLW
HsNEU2   1   -MASLPVLQKES-------------------------------------------VFQSGAH---
HsNEU3   1   -MEEVTTCSFNS-------------------------------------------PLFRQEDDRG
HsNEU4   1   --MGVPRTPSRT-------------------------------------------VLFERER-TG

HsNEU1   66  VSGRQIGSVDTFRIPLITATPRG-TLLAFAEARKMSSSDEGAKFIALRR----SMDQGSTWSPTA
HsNEU2   19  ----------AYRIPALLYLPGQQSLLAFAEQR-ASKKDEHAELIVLRRGDYDAPTHQVQWQAQE
HsNEU3   22  I---------TYRIPALLYIPPTHTFLAFAEKR-STRRDEDALHLVLRRG--LRIGQLVQWGPLK
HsNEU4   20  L---------TYRVPSLLPVPPGPTLLAFVEQR-LSPDDSHAHRLVLRRG--TLAGGSVRWGALH

HsNEU1   126 FIVNDGDVPDGLNLGAVVSDVETGVVFLFYS-LCAHK-AGCQVASTM------LVWSKDDGVSWS
HsNEU2   73  VVAQARLDGHRSMNPCPLYDAQTGTLFLFFIAIPGQVTEQQQLQTRANVTRLCQVTSTDHGRTWS
HsNEU3   75  PLMEATLPGHRTMNPCPVWEQKSGCVFLFFICVRGHVTERQQIVSGRNAARLCFIYSQDAGCSWS
HsNEU4   73  VLGTAALAEHRSMNPCPVHDAGTGTVFLFFIAVLGHTPEAVQIATGRNAARLCCVASRDAGLSWG

HsNEU1   183 TPRNLSLD-IGTEV-----FAPGPGSGIQKQREPRKGRLIVCGHGTLERD-------------GV
HsNEU2   138 SPRDLTDAAIGPAYREWSTFAVGPGHCLQLND--RARSLVVPAYAYRKL------HPIQRPIPSA
HsNEU3   140 EVRDLTEEVIGSELKHWATFAVGPGHGIQLQS----GRLVIPAYTYYIPSWFFCFQLPCKTRPHS
HsNEU4   138 SARDLTEEAIGGAVQDWATFAVGPGHGVQLPS----GRLLVPAYTYRVD-RRECFGKICRTSPHS

HsNEU1   229 FCLLSDDHGASWRYGSGVSGIPYGQPKQENDFNPDECQPYELPDGS----VVINARNQNNYHCHC
HsNEU2   195 FCFLSHDHGRTWARGHFVA------------QDTLECQVAEVETG-EQRVVTLNARSHLRA----
HsNEU3   201 LMIYSDDLGVTWHHGRLIRP-----------MVTVECEVAEVTGRAGHPVLYCSARTPNRC----
HsNEU4   198 FAFYSDDHGRTWRCGGLVPN-----------LRSGECQLAAVDGGQAGSFLYCNARSPLGS----

HsNEU1   290 ---RIVLRSYDACDTLRPRDVTFDP------ELVDPVVAAG-----------------------
HsNEU2   243 ---RVQAQSTNDGLDFQESQLVKKLVEPPPQGCQGSVISFPSPR--------------SPAQ---
HsNEU3   251 ---RAEALSTDHGEGFQRLALSRQLCEP-PHGCQGSVVSFRPLEIPHRCQDSSSKDAPTIQQSSP
HsNEU4   248 ---RVQALSTDEGTSFLPAERVASLPET-AWGCQGSIVGFPAPAPNRPRDDSWSVGPRSPLQPPL

HsNEU1   322 ------------------------------------------------------------AVVTS
HsNEU2   -   ------------------------------------------------------------
HsNEU3   315 GSSLRLEEE-------------------------------------------------AGTPS
HsNEU4   312 LGPGVHEPPEEAAVDPRGGQVPGGPFSRLQPRGDGPRQPGPRPGVSGDVGSWTLALPMPFAAPPQ

HsNEU1   329 SG-IVFFSNPAHPEFRVNLTLRW--SFSNGTSWRKETVQLWPGPSGYSSLATLEGSMDGEEQAPQ
HsNEU2   292 ---WLLYTHPTHSWQRADLGAYLNPRPPAPEAWSEPVLLAK-GSCAYSDLQSMGTGPDGS---PL
HsNEU3   328 ES-WLLYSHPTSRKQRVDLGIYLNQTPLEAACWSRPWILHC-GPCGYSDLAALE--EEG-----L
HsNEU4   377 SPTWLLYSHPVGRRARLHMGIRLSQSPLDPRSWTEPWVIYE-GPSGYSDLASIGPAPEGG---LV

HsNEU1   389 LYVLYEKGRNHYTESISVAKISVYGTL-----------------------
HsNEU2   353 FGCLYEAN---DYEEIVFLMFTLKQAFPAEY--------------------
HsNEU3   385 FGCLFECGTKQECEQIAFRLFTHREILSHLQGDCTSP--GRNPS--QFKSN
HsNEU4   438 FACLYESGARTSYDEISFCTFSLREVLENVPASPKPPNLGDKPRGCCWPS-
```

Fig. 1. Sequence alignment of four types of human sialidase enzymes. Identical and similar residues are shown on a light blue and a gray background, respectively. The conserved Y/FRI/VP motifs are overlined in black and the Asp boxes are underlined in black. The active site amino acid residues corresponding to the active site of HsNEU2 derived from crystallographic data are shown in bold with red color [32]. The NEU symbol prefixed with Hs, which indicates *Homo sapiens* species. Amino acid residues not included to the model are rendered in italics.

model of a protein sequence automatically and rapidly, based on a given sequence alignment to a known 3D protein structure. MODELER employs probability density functions (PDFs) as the spatial restraints rather than energy [34]. The PDFs that are used in restraining the model structure are derived analytically using statistical mechanics and empirically using a database of known protein structures. The geometry of loop regions was corrected using MODELER/Refine Loop command. The non-selective inhibitor (DANA) present in a half-chair conformation at the active site of experimental complex of structure of NEU2 was copied into active site of the model structures. The two bound water molecules (Wat129 and Wat131) within 5 Å distance from DANA in the crystal structure of NEU2 were also included in the models. Obtained complexes were minimized using *DS CHARMm* module. The atom types were assigned using the CHARMM forcefield and the distance-dependent dielectric constant 4 was employed for approximate solvent effects. The calculation included 100 steps of steepest descent (SD) minimization followed by 100 steps of an unconstrained MD simulation (The Verlet leapfrog integration method with temperature coupling) at 300 K with a time step of 1.0 fs. The non-bonded cut-off was set to 14 Å. Finally 100 steps of conjugated gradient (CG) minimization was performed without any constraint.

2.4. Model validation

Energy-minimized models were assigned to pH 7.4, which resulted in a +1 charge for arginines and lysines, −1 charge for the aspartates and glutamates using *DS Biopolymer* module. The bond angle, secondary structure, residue contact and hydrophobicity of the models were analyzed using protein report of the same module. The stereochemical, volume and surface properties of the models were evaluated by PROCHECK [35], WHAT IF [36] and PROVE [37], available at Biotech Validation Suite for Protein Structures (http://biotech.ebi.ac.uk:8400/). Fitness of the models sequence in their current 3D environment was evaluated by Profiles-3D/Verify [38] of *DS protein health* module. The root mean square deviation (RMSD) between the main chain atoms of the models and template was calculated for the reliability of the models. Finally, the best quality model from NEU1, NEU3 and NEU4 was chosen for further calculations and molecular modeling studies.

2.5. Molecular electrostatic potential (MEP)

The electrostatic potential around the template and the modeled molecular systems was calculated by solving nonlinear Poisson–Boltzmann equation using finite difference method [39] as implemented in the *DS DelPhi* module. The potential was calculated on grid points per side (65, 65, 65) and the 'grid fill by solute' parameter was set to 80%. The dielectric constants of the solvent and the solute were set to 80.0 and 2.0, respectively. An ionic exclusion radius of 2.0 Å, a solvent radius of 1.4 Å and a solvent ionic strength of 0.145 M were applied. CHARMM charges and radii were used for this calculation. The solvent exposure was calculated using the Connolly algorithm with a probe of 1.4 Å radius [40].

3. Results and discussion

3.1. Homology models of NEU1, NEU3 and NEU4

There are many examples where homology modeling techniques have supported the drug discovery process especially in the target identification and/or validation, lead identification as well as lead optimization with respect to potency and selectivity [41]. The extent of information derived from the homology model depends on the quality of the model. Since the accuracy of the homology model is related to the degree of sequence identity and similarity between the template and target, template search and sequence alignment is a crucial step in any homology modeling [42]. For this reason extreme caution was taken into consideration, while searching for the template and while aligning the sequences. As a result of Gapped-BLAST-based template search through PDB, the crystal structure of NEU2 (PDB CODE: 1VCU, Chain B) was selected unanimously as the template. NEU2 has a high level of sequence identity with NEU3 (42%) and NEU4 (44%) and low but significant identity with NEU1 (28%). Since human sialidase enzymes have low homology with their viral, bacterial and protozoal counterparts, the models built with them may not be accurate. Moreover NEU2 is the only human sialidase whose crystal structure is available so far, and hence we biased NEU2 as an active template for the quality of the model. As we aimed to model the ligand-bound conformation of proteins, we sought the crystal structure of the human NEU2 in complex with the inhibitor DANA instead of NEU2 apo-form (PDB CODE: 1SNT). The multiple sequence alignment of human sialidase enzymes was done to get optimal alignment of human family members and then corrected manually (Fig. 1). The alignment of sequences showed the common motif F/YRI/VP near N-terminal and the highly conserved amino acids residues that form the active site of NEU2 enzyme. The amino acid sequences of NEU1, NEU3 and NEU4 were aligned with NEU2 individually on the basis of multiple alignment as obtained above, followed by a few manual adjustments for the final model construction. The residues of low homology regions M1 to D50 of NEU1, P288 to S309 and S314 to T323 of NEU3 and P286 to Q373 of NEU4 were removed from the alignment assuming that these regions should not have a drastic influence on the active site modeling since these residues are far away from the active site region. The refined final alignments were used for constructing homology models of human sialidase enzymes using the MODELER program. MODELER generates a large number of template-derived restraints to force the model towards the structure of the template and converges to the best possible structure by simultaneously satisfying a network of spatial restraints and molecular geometry using the CHARMM forcefield. The optimization process to generate the model consists of applying the variable target function as well as conjugate gradients and molecular dynamics with simulated annealing. Approximately 25 homology models were built for

each enzyme following which the non-selective inhibitor (DANA) and two buried bound water molecules (Wat129 and Wat131) were placed in the active site of the models. To fix the DANA in the correct position, interatomic distances between DANA and protein atoms were adjusted. The low homology loops near the active site regions of NEU1 (G245 to N261), NEU3 (I183 to T196) and NEU4 (V181 to T193) were refined to access proper folding with minimum steric clash. The possible unfavourable interactions between the models and DANA were minimized with minimum steps of Steepest Descent minimization and MD simulation followed by Conjugate Gradient minimization. Many attempts were made in an effort to minimize the obtained complexes; however, no significant improvements were obtained beyond that resulting from minimum steps of minimization and dynamics simulation without affecting the stereochemical properties of the models. Then, the energy-minimized conformers were subjected into various protein analyses as mentioned in the methods section. Finally, the best model obtained from each human sialidase enzyme was chosen for further modeling.

The Ramachandran plots for local backbone conformation of each residue in the final models were produced by PROCHECK [35]. In NEU3 model, Φ and Ψ dihedral angles of 99.4% of residues were located within the allowed regions (82% most favoured) of the Ramachandran plot. While in NEU4, 85% (260 residues) were in the most favoured regions with only 1.3% (4 residues) in disfavoured regions. In NEU1, 75% (230 residues) were in the most favoured regions with only 2% (6 residues) in disfavoured regions. The 1D–3D compatibility score (Profiles-3D score) of NEU1, NEU3 and NEU4 were 128,155 and 165, respectively, compared with the expected high scores of 165, 165 and 175 and the expected low scores of 79, 89 and 80, respectively. The root mean square deviation (RMSD) values of the residue Cα atoms of NEU2 with NEU1, NEU3 and NEU4 were 2.24 Å (332 residues), 0.77 Å (364 residues) and 0.47 Å (366 residues), respectively. The above results express the strong confidence in the homology models. Although NEU1 was constructed with 28% sequence similarity, the active site and the neighboring residues have been modeled with accuracy for the useful

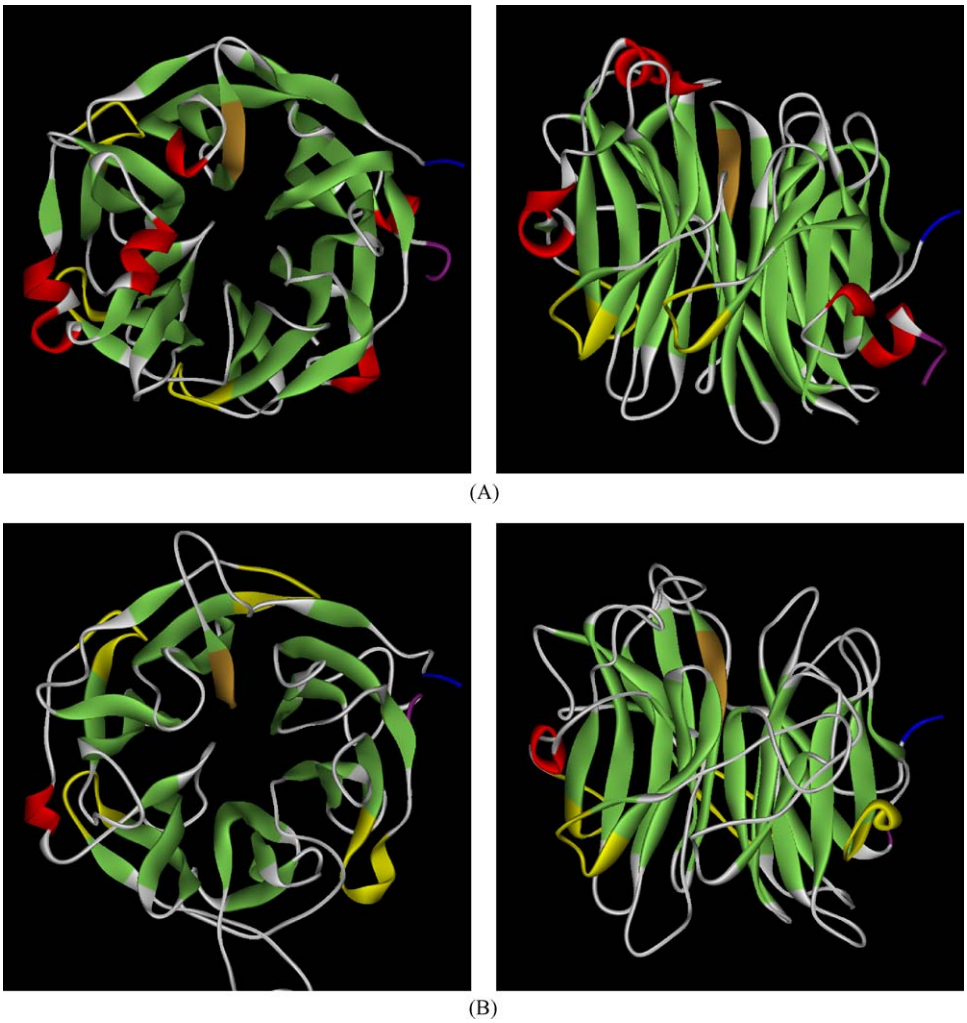

Fig. 2. Orthogonal view of experimental NEU2 structure (A) and predicted structures of NEU1 (B), NEU3 (C) and NEU4 (D). The ribbon diagram shows top view (left) and lateral view (right) of human sialidases. The secondary structure elements of proteins are defined by the Kabsch and Sander method. The β-strands are colored in light green, the α helices in red. The N and C terminals are indicated by blue and violet, respectively. The conserved Y/FRI/VP and Asp boxes are shown in orange and yellow, respectively.

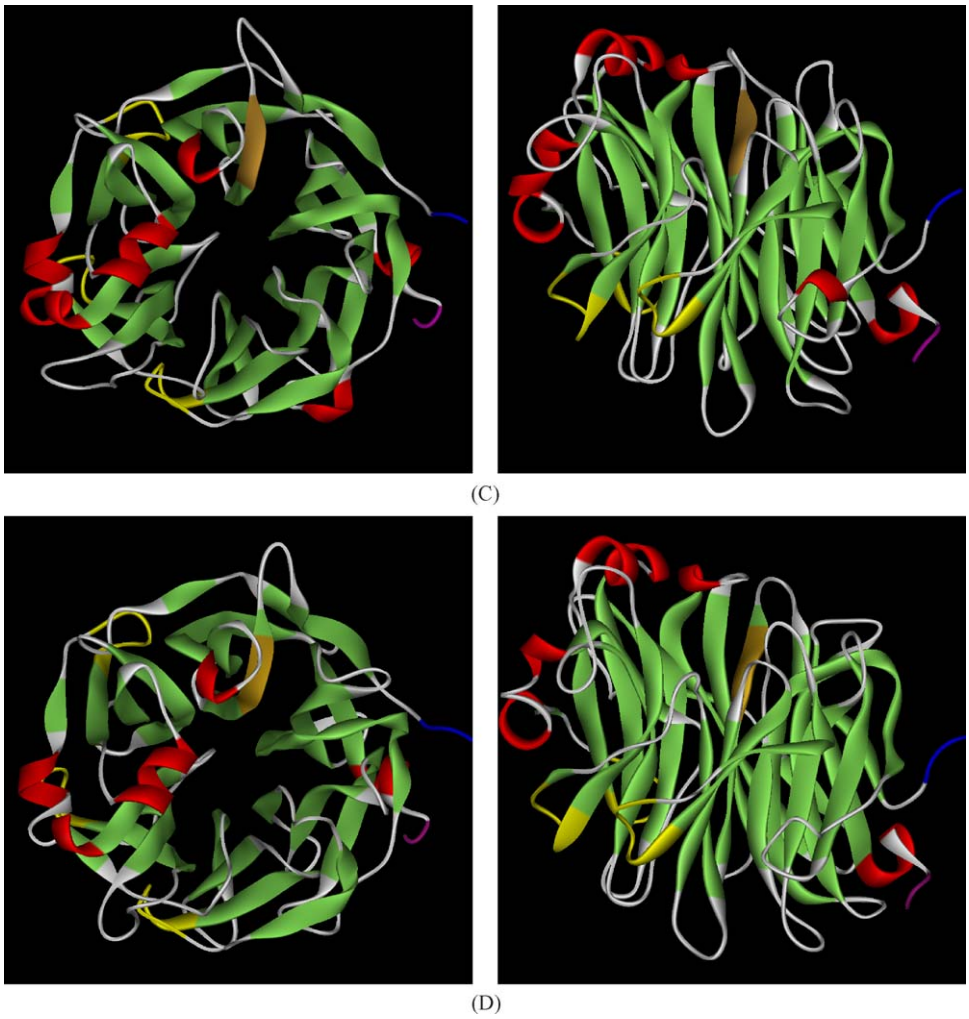

(C)

(D)

Fig. 2. (*Continued*).

comparison with other human sialidases. The RMSD of active site residue Cα atoms between NEU2 and NEU1 is 0.86 Å (23 residues) at 5 Å level, confirms reliability of the NEU1 model.

The final structures of NEU1, NEU3 and NEU4 along with the template NEU2 are presented in Fig. 2. The secondary structures of modeled proteins are defined by the Kabsch and Sander method [43]. The known 3D-structure of the NEU2 complex comprises of six-bladed β-propeller fold with 25 β-strands, 5 α-helices and 26 connecting segments arranged around the axis passing through the active site [32]. Likewise, the predicted model of NEU1 appears to fold into 22 β-strands, 2 α-helices and 25 connecting segments. The NEU3 model has 24 β-strands, 6 α-helices and 27 connecting segments and the NEU4 model is made up of 25 β-strands, 5 α-helices and 29 connecting segments. The typical Asp boxes and F/YRI/VP motifs are arranged in topologically equivalent positions to each other. The N- and C-terminal have been arranged outside the β-propeller i.e. opposite site of the active site crevice and close to each other as observed in NEU2. The overall structure of predicted proteins and experimental NEU2 shows common 3D-fold, but variation arises in two ways, as already observed with bacterial and viral neuraminidases [44]. The first variation is the twist of β-strands and its relative arrangement to the propeller axis and the other variation is the change in conformations of the loops connecting the β-strands. The variable loops on the catalytic surface region are considered to be of great importance, as they appear to be involved in substrate/inhibitor recognition. As observed in the crystal structure of NEU2, two disordered loops in the apo-form become ordered to form α1 and α2 upon inhibitor binding (induced fit behavior) [32], suggesting that the loops are considered to exist as loose conformations and it can adopt wide range of conformations according to the operating environment. The length and conformation of the loops in the active site surface may be in fact responsible for substrate specificity. A close examination of human sialidase models reveals that all the topological features belong to the sialidase superfamily.

3.2. Active site modeling

The structural differences in the active site amongst human sialidase enzymes are of particular interest, especially for the design of compounds that would potentially have greater

affinity for the NEU3 enzyme active site. Active site crevice of predicted enzymes is organized in the center of the β-propeller fold in the same fashion as in bacterial and viral neuramindases [44]. In order to compare the active sites of human sialidases, the binding pocket is defined as a subset that contains residues in which any atom lies within 5.0 Å from the inhibitor, DANA. Protein–DANA contacts were determined using the LPC www-server (http://bip.weizmann.ac.il/oca-bin/lpccsu) [45]. The binding mode of DANA in the active site of template NEU2 and in the other predicted models is given in Fig. 3. Putative hydrogen bonds and hydrophobic contacts between human sialidases and inhibitor (DANA) are presented in Table 1. The four common functional groups of sialic acid (recognition portion of the sialoglycoconjugate substrate) or inhibitor DANA (a sialic acid transition-state analog) that bind to the enzyme active site are the 2-carboxylate, 4-hydroxyl, 5-N-acetyl and 6-glycerol moiety (Fig. 4). DANA binding residues of NEU2 are mostly preserved in the active site crevice of all three modeled human sialidases except for a few residues. This observation represents the striking evolutionary 3D convergence among the human family members. It has also been shown previously that the 5-*N*-acetyl and 6-glycerol binding groups of experimental structure of NEU2 are not shared by bacterial and viral neuraminidases [32], suggesting that sialidases have evolved ingeniously to adopt their functioning environment [44].

As seen in the crystal structure of NEU2, the arginine triad (R21 R237 R304) that binds to 2-carboxylate and a tyrosine residue (Y334), which stabilizes the sialyl–enzyme intermediate during catalysis [46], are highly conserved in the same positions of all modeled structures (R78 R280 R341 and Y370 in NEU1, R25 R245 R340 and Y370 in NEU3, R23 R242 R389 and Y419in NEU4). Two other amino acid residues in NEU4 (Y447 and W274) and one residue in NEU3 (H277) are in addition, interacting with the 2-carboxylate group of inhibitor (DANA). The two acidic

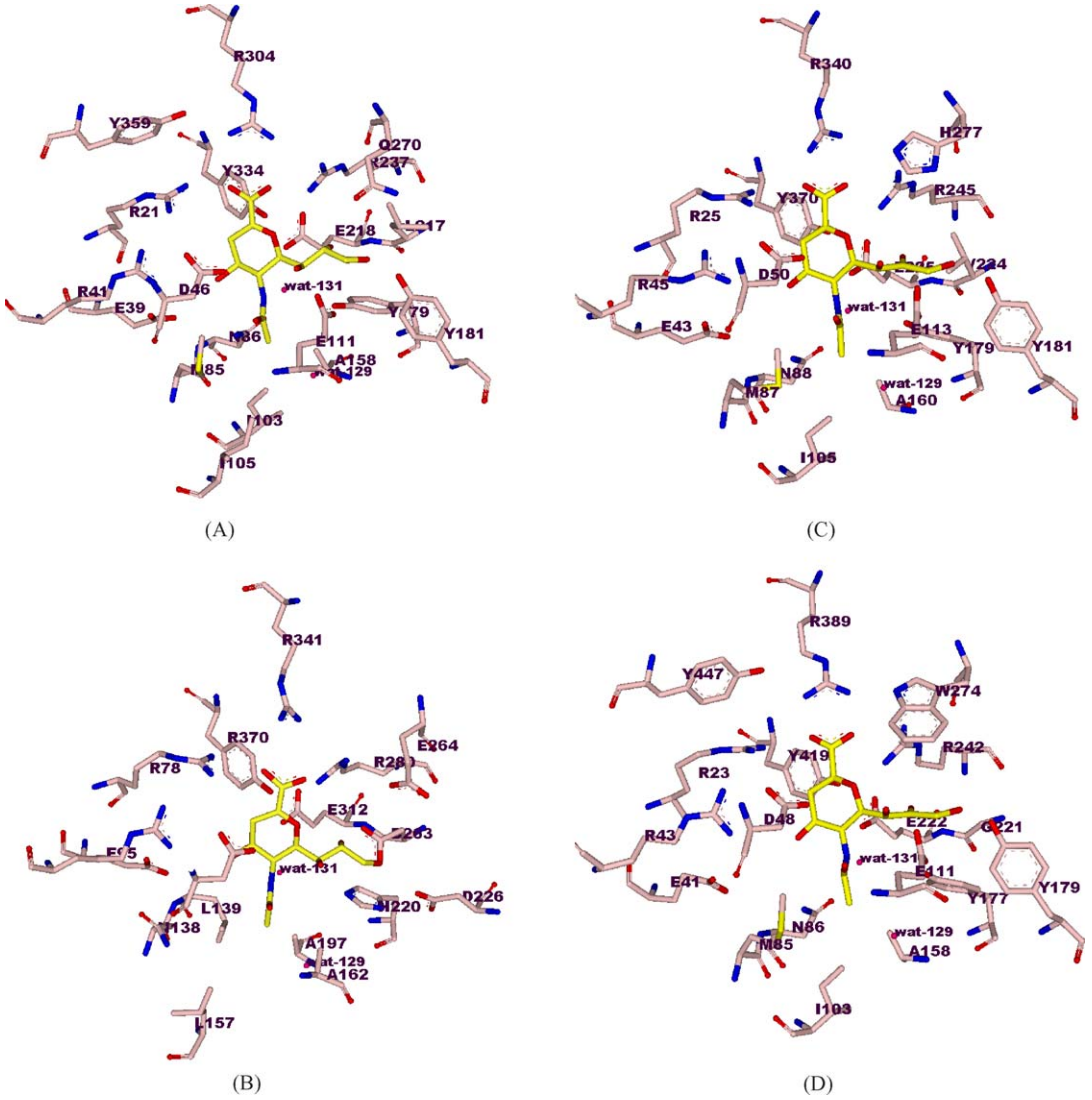

Fig. 3. The binding mode of DANA in the active site of template NEU2 (A) and models NEU1 (B), NEU3 (C), NEU4 (D) at 5 Å distance level. DANA and contact residues are depicted in stick mode. Carbon atoms are colored yellow for DANA and light pink for protein; oxygen atoms, red; nitrogen atoms, blue; sulfur atoms, yellow for protein. Water molecules are rendered as magenta spheres.

Table 1
Putative hydrogen bonds and hydrophobic contacts between human sialidases and inhibitor's (DANA) functional groups—the contacts are inferred from the known crystal structure of NEU2 (template) and the predicted 3D models

DANA's constituents	Template	Models		
	NEU2	NEU1	NEU3	NEU4
2-Carboxylate				
O1A	R21 R304 Y334	R78 R341 Y370	R25 R340 Y370	R23 R389 Y419
O1B	R237 R304 Y334	R280 R341	R245 R340 H277	R242 R389 W274, Y447
4-Hydroxyl				
O4	E39 R41 D46 N86	E95 R97 D103 N138	E43 R45 D50 N88	E41 R43 D48 N86
5-*N*-acetyl				
N5	N86 Y179 E218 D46 Wat131	D103 E312 Wat131	N88 Y179 E225 D50 Wat131	N86 Y177 E222 D48 Wat131
O10	M85[a]	–	M87[a]	M85[a]
C10	M85[a] I103[a]	L139[a]	M87[a] I105[a]	M85[a] I103[a]
C11	I105[a] A158[a]	L139[a] L157[a] A162[a] A197[a]	A160[a]	A158[a]
Glycerol				
C9	L217[a]	H220[a]	V224[a] H277[a]	W274[a]
O7	D46 E111	H220 E264	D50 E113	D48 E111
O8	Y179 E218 R237	D263 R280 E312	Y179 E225 R245	Y177 E222 R242
O9	E111 Y179 Y181 Q270	D226 D263	E113 Y179 Y181 H277	E111 Y177 Y179 W274

[a] Indicates residue involved in hydrophobic contact.

residues D46/E218 in NEU2 are acting as an enzymatic acid–base catalyst during hydrolysis [47], are also arranged in comparable spatial distances in the models (D103/E264 in NEU1, D50/E225 in NEU3, D48/E222 in NEU4). The four amino acid residues (D, E, R, and N) that interact with 4-hydroxyl are same in all active sites. The 5-*N*-acetyl coordinating residues of NEU3 and NEU4 are identical with the experimental structure of NEU2 in an equivalent spatial arrangement, where as NEU1 shows striking variation in this region. Four out of five amino acid residues of NEU1 (L139, L157, A162 and A197) that define the hydrophobic pocket occupied by 5-*N*-acetyl of inhibitor, are different from other human sialidases. As observed in NEU2, the amido N5 of 5-*N*-acetyl is hydrogen bonded with the buried water-131, and this water molecule in turn interacts with three amino acid residues (N86 Y179 E218 of NEU2, N88 Y179 E225 of NEU3, N86 Y177 E222 of NEU4) and another water-129 forms hydrogen bonds with a glutamate residue (E111 of NEU2, E113 of NEU3, E111 of NEU4); while in NEU1, water-131 interacts with H220 and E312, and water-121 interacts with H220 and backbone of A162. C9 of the 6-glycerol moiety of NEU2 in crystal structure forms hydrophobic contact with L217, while in NEU1 with H220, in NEU3 with V224 and H227 and in NEU4 with W274. Likewise O7 forms hydrogen bonding with D46 and E111 of NEU2, while in NEU1 with H220 and E264, in NEU3 with D50 and E113 and in NEU4 with D48 and E111. O8 forms hydrogen bonds with identical residues of NEU2, NEU3 and NEU4 (R, Y and E), but with D263, R280 and E312 of NEU1. Similarly O9 forms hydrogen bonds with identical residues of NEU2, NEU3 and NEU4 (Y, Y and E), but with D263 and D226 of NEU1. In addition, O9 is also involved in hydrogen bonding with Q270 of NEU2, in NEU3 with H277 and in NEU4 withW274. These relative differences in the active site of human sialidases will definitely affect the steric and electrostatic potential as well as hydrogen bonding interactions with inhibitors and giving new suggestions for the design of selective NEU3 inhibitors.

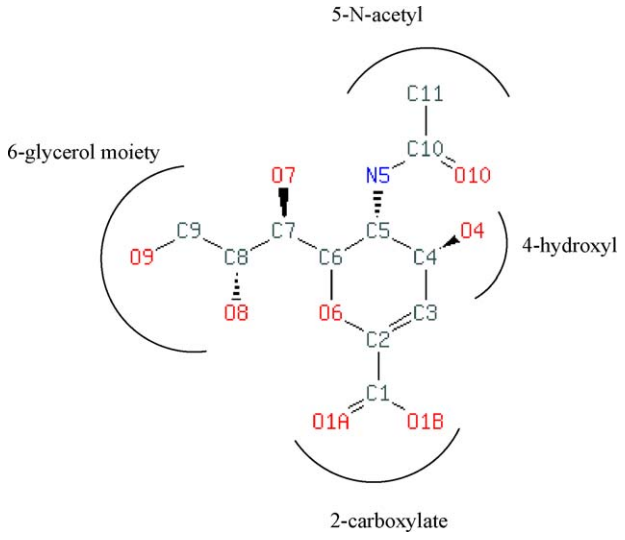

Fig. 4. Schematic representation of DANA and its four constituent groups required for binding.

Site-directed mutagenesis studies on NEU1 [48] and NEU3 [49] were carried out previously. Although the mutated residues were not exactly the same as predicted active site residues, mutants adjacent to active site can affect the enzymatic activity by misfolding the β-strand structures that disturbs active site architecture.

Active site crevice of NEU3 and NEU4 models are more similar to template NEU2 than to NEU1 model. This difference results in different complementary contact surface, which affects substrate recognition. This may be the reason for the inability of NEU1 to hydrolyze gangliosides, while NEU2, NEU3 and NEU4 can hydrolyze the gangliosides very efficiently under standard enzyme assay conditions. Furthermore, NEU3 enzymatic activity is specific to gangliosides only; although the reason behind that remains unclear. This is possibly due to steric hindrance in the vicinity of NEU3 active site, making it unable to recognize the chemical connectivity of sialoglycoconjugates other than gangliosides. Notably, active site volume of NEU3 is smaller (216 $Å^3$) than active site of other human sialidases (277 $Å^3$ for NEU1, 227 $Å^3$ for NEU2 and 242 $Å^3$ for NEU4), which might help for designing selective inhibitors.

3.3. Molecular electrostatic potential (MEP)

The MEP is an electrical effect of the electrons and nuclei of a molecule in its vicinity [50]. Protein electrostatic potential is an indicator of electrostatic properties that are evolutionally selected by a protein to perform a specific function [51]. The electrostatic potential of proteins caused by side chains of polar and charged residues plays a role in protein folding and stability, enzyme catalysis and specific protein–protein or protein–ligand recognition. The computer graphics representation of the molecular surface electrostatic potential is a powerful tool for studying intermolecular specificity because it facilitates the simultaneous search for both steric and electrostatic complementarity in protein–ligand interactions [52]. Therefore examining the potential for electrostatic complementarity of the protein–ligand complex among the human sialidase models can be a useful technique for the design of specific inhibitors.

The calculated electrostatic potential mapped on to the solvent accessible surface of the models and the template is presented for comparison in Fig. 5. The MEP values on the surfaces of human sialidases range from −303 to +239 kcal/mol Å

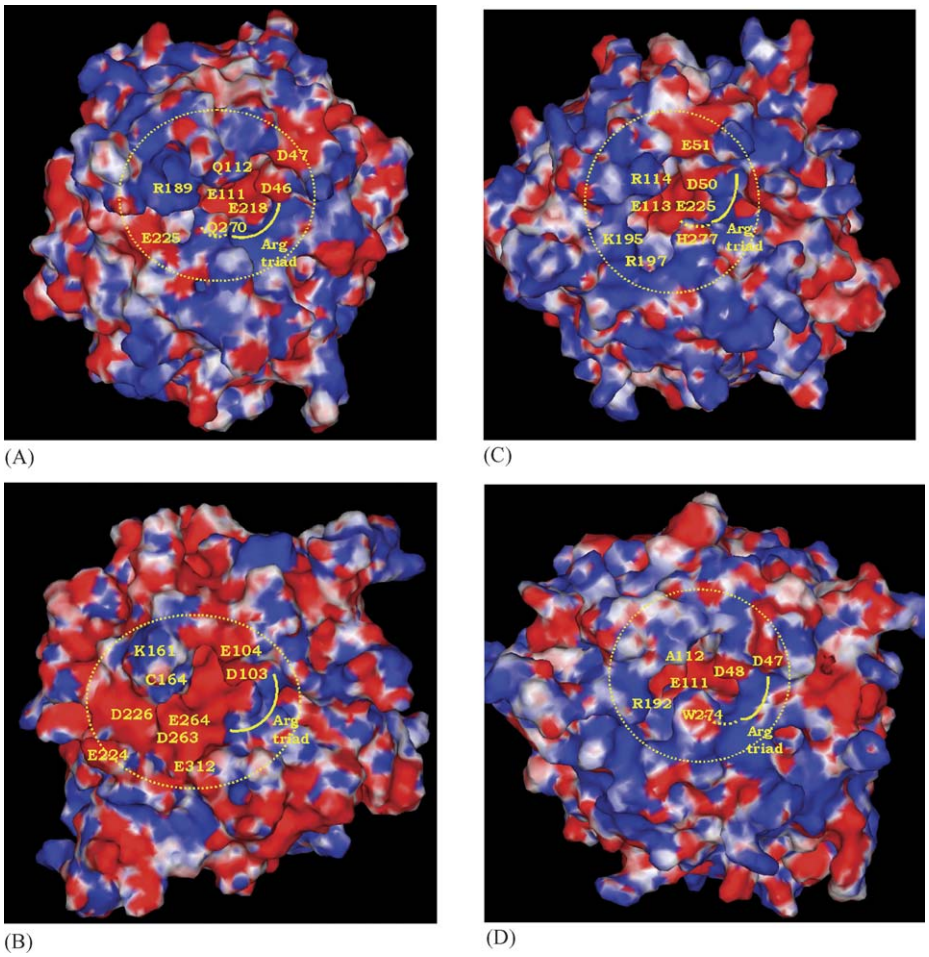

Fig. 5. The electrostatic potential map of human sialidases. Solvent accessible surface of models NEU2 (A), NEU1 (B), NEU3 (C) and NEU4 (D) show the Delphi electrostatic potentials. Positive potentials are shown in blue, negative potentials in red and neutral in white. The yellow circle with dotted lines indicates the active site entry. Surface residues vicinal to active site are labeled on the map.

for template NEU2, −296 to +241 kcal/mol Å for NEU1, −331 to +259 kcal/mol Å for NEU3 and −267 to +253 kcal/mol Å for NEU4. The ranges of electrostatic potential are not differing greatly but at the same time, the striking differences have been observed in the local disposition of the charged groups. The putative substrate entry site in NEU1 is more negative than others. But in the case of NEU3, it is found to be more positive than others. All human sialidases show similar positive MEP value in 2-carboxylate binding region might be due to conserved arginine triad. An acidic deep cleft having high negative potential flanked by Asp residue has also been observed in all three-enzyme models and the template. The presence of E224, D226, E263 and E264 in NEU1, makes a highly negative potential region value around the active site. While in NEU3, the same region is covered by high positive potential due to K195 and R197 along with a small negative potential patch near arginine triad occupied by H277. In NEU2, near to glycerol-binding region has high positive MEP value due to presence of R189 while adjacent E225 has high negative MEP value. The same region in NEU4 is also found to be having high positive potential area due to R192 with slight pinches of neutral and negative potentials. W274 of NEU4 proximal to arginine triad gives rise to negative potential around that region. These differences in the electrostatic potential where the substrate is likely to enter the active site could be responsible for experimentally determined differences in the substrate specificity. An important contribution to support this fact comes from site directed mutation studies on NEU3 [49], which indicated that mutation on R114Q decreased the hydrolysis of GD3 and GD1a, but increased the ability of the enzyme to hydrolyze the GM2 (which is poor substrate for wild-type), whereas mutation on R114A enhanced the activity towards GD3 and GD1a (chemical structures of GD3, GM2 and GD1a are shown in Fig. 6). Interestingly, the spatial position of R114 in predicted NEU3 structure is found to be in the entrance to the active site and it is replaced by Q112 in crystal structure NEU2 and A112 in predicted NEU4 structure, respectively. The variations in these amino acid residues show difference in

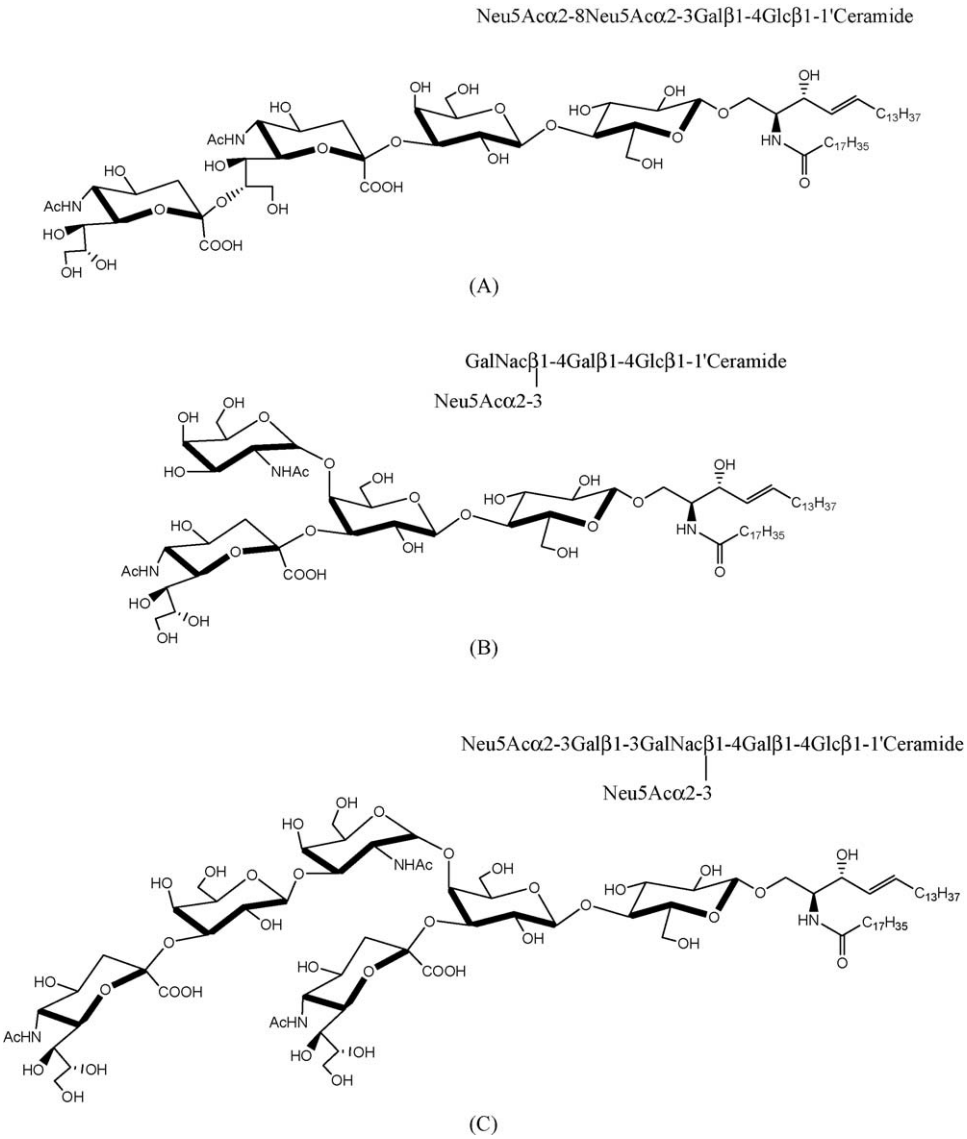

Fig. 6. Schematic formula and 2D structure of gangliosides: (A) GD3; (B) GM2; (C) GD1a.

electrostatic potential across this region (shown in Fig. 5). These observations suggest that R114Q mutant of NEU3 might change the electrostatic potential from negative to positive; this shifts the substrate specificity similar to that of NEU2, which has a small positive potential patch in this region. Similarly, R114A mutant of NEU3 might create a fleck of non-polar area, which makes it more suitable for hydrolysis of GD1a than wild-type and induces it to behave like NEU4 [24], which has the same non-polar patch in that region. The present findings of electrostatic potential differences at the active site surface of human sialidase enzymes is of particular interest in the design of compounds with greater affinity for the NEU3.[1]

4. Conclusion

Aberrant expression of sialidases and its possible significance in cancer has been studied. Recent progress in cloning and characterization of sialidases at molecular level has revealed the molecular mechanisms of alterations during carcinogenesis. In particular, increased expression of plasma membrane associated sialidase (NEU3) in cancer cells leads to protection against apoptosis, probably via modulation of gangliosides. NEU3 over expression is also implicated in the development of insulin resistance. Hence selective NEU3 inhibition would be a new therapeutic approach in cancer as well as in insulin-resistant diabetes. Here we have constructed the homology model of NEU1, NEU3 and NEU4 by using experimental crystal structure of NEU2. Comparison between the modeled structures and crystal structure of NEU2 showed similarity in active site topology and overall folding of enzymes. Despite these similarities, some differences at the active site and its vicinity emphasize the differences in the experimental substrate specificity. Molecular electrostatic potential calculations revealed the differences in the charge distributions around the putative substrate entry site, which can account for differential substrate recognition and binding. Thus results of this study supply useful information in better understanding of the structural differences at the active site among the human sialidase enzymes and the present work constitutes the first step in the structure-based design of selective NEU3 inhibitors.

Acknowledgements

The first author (SM) is grateful to Ministry of Education, Culture, Sports, Science and Technology, Government of Japan (MEXT) for the financial support, No. 042271. This work was supported in part by Grants-in-Aid (No. 17101007) for Scientific Research from MEXT and by CREST of JST (Japan Science and Technology Corporation) to MK. The authors are thankful to Ms. Subashree and Mrs. Sativa for many valuable discussions during the preparation of manuscript.

[1] *Note*: During the preparation of this manuscript we became aware of a related report on tertiary structure prediction on NEU3 and NEU4 [53].

References

[1] E. Monti, A. Preti, B. Venerando, G. Borsani, Recent development in mammalian sialidase molecular biology, Neurochem. Res. 27 (2002) 649–663.
[2] K.E. Achyuthan, A.M. Achyuthan, Comparative enzymology, biochemistry and pathophysiology of human exo-α-sialidases (neuraminidases), Comp. Biochem. Physiol. B: Biochem. Mol. Biol. 129 (2001) 29–64.
[3] E. Bonten, S.A. Van der, M. Fornerod, G. Grosveld, A. d'Azzo, Characterization of human lysosomal, neuraminidase defines the molecular basis of the metabolic storage disorder sialidosis, Genes Dev. 10 (1996) 3156–3169.
[4] A.V. Pshezhetsky, C. Richard, L. Michaud, S. Igdoura, S. Wang, M.A. Elsliger, J. Qu, D. Leclerc, R. Gravel, L. Dallaire, M. Potier, Cloning, expression and chromosomal mapping of human lysosomal sialidase and characterization of mutations in sialidosis, Nat. Genet. 15 (1997) 316–320.
[5] E. Monti, A. Preti, E. Rossi, A. Ballabio, G. Borsani, Cloning and characterization of NEU2, a human gene homologous to rodent soluble sialidases, Genomics 57 (1999) 137–143.
[6] E. Monti, A. Preti, C. Nesti, A. Ballabio, G. Borsani, Expression of a novel human sialidase encoded by the NEU2 gene, Glycobiology 9 (1999) 1313–1321.
[7] E. Monti, M.T. Bassi, N. Papini, M. Riboni, M. Manzoni, B. Venerando, G. Croci, A. Preti, A. Ballabio, G. Tettamanti, G. Borsani, Identification and expression of NEU3, a novel human sialidase associated to the plasma membrane, Biochem. J. 349 (2000) 343–351.
[8] T. Wada, Y. Yoshikawa, S. Tokuyama, M. Kuwabara, H. Akita, T. Miyagi, Cloning, expression, and chromosomal mapping of a human ganglioside sialidase, Biochem. Biophys. Res. Commun. 261 (1999) 21–27.
[9] E. Monti, M.T. Bassi, R. Bresciani, S. Civini, G.L. Croci, N. Papini, M. Riboni, G. Zanchetti, A. Ballabio, A. Preti, G. Tettamanti, B. Venerando, G. Borsani, Molecular cloning and characterization of NEU4, the fourth member of the human sialidase gene family, Genomics 83 (2004) 445–453.
[10] T. Miyagi, K. Kato, S. Ueno, T. Wada, Aberrant expression of sialidase in cancer, Trends Glycosci. Glycotechnol. 16 (2004) 371–381.
[11] P. Roggentin, R. Schauer, L.L. Hoyer, E.R. Vimr, The sialidase superfamily and its spread by horizontal gene transfer, Mol. Microbiol. 9 (1993) 915–921.
[12] V. Seyrantepe, K. Landry, S. Trudel, J.A. Hassan, C.R. Morales, A.V. Pshezhetsky, Neu4, a novel human lysosomal lumen sialidase, confers normal phenotype to sialidosis and galactosialidosis cells, J. Biol. Chem. 279 (2004) 37021–37029.
[13] A.V. Pshezhetsky, M. Ashmarina, Lysosomal multienzyme complex: biochemistry, genetics, and molecular pathophysiology, Prog. Nucl. Acid. Res. Mol. Biol. 69 (2001) 81–114.
[14] V. Seyrantepe, H. Poupetova, R. Froissart, M.T. Zabot, I. Maire, A.V. Pshezhetsky, Molecular pathology of NEU1 gene in sialidosis, Hum. Mutat. 22 (2003) 343–352.
[15] K. Gee, M. Kozlowski, A. Kumar, Tumor necrosis factor-alpha induces functionally active hyaluronan-adhesive CD44 by activating sialidase through p38 mitogen-activated protein kinase in lipopolysaccharide-stimulated human monocytic cells, Biol. Chem. 278 (2003) 37275–37287.
[16] N.M. Stamatos, F. Liang, X. Nan, K. Landry, A.S. Cross, L.X. Wang, A.V. Pshezhetsky, Differential expression of endogenous sialidases of human monocytes during cellular differentiation into macrophages, FEBS J. 272 (2005) 2545–2556.
[17] C. Tringali, N. Papini, P. Fusi, G. Croci, G. Borsani, A. Preti, P. Tortora, G. Tettamanti, B. Venerando, E. Monti, Properties of recombinant human cytosolic sialidase HsNEU2. The enzyme hydrolyzes monomerically dispersed GM1 ganglioside molecules, J. Biol. Chem. 279 (2004) 3169–3179.
[18] K. Sato, T. Miyagi, Involvement of an endogenous sialidase in skeletal muscle cell differentiation, Biochem. Biophys. Res. Commun. 221 (1996) 826–830.

[19] A. Fanzani, R. Giuliani, F. Colombo, D. Zizioli, M. Presta, A. Preti, S. Marchesini, Overexpression of cytosolic sialidase Neu2 induces myoblast differentiation in C2C12 cells, FEBS Lett. 547 (2003) 183–188.
[20] K.T. Ha, Y.C. Lee, S.H. Cho, J.K. Kim, C.H. Kim, Molecular characterization of membrane type and ganglioside-specific sialidase (Neu3) expressed in *E. coli*, Mol. Cells 17 (2004) 267–273.
[21] C. Oehler, J. Kopitz, M. Cantz, Substrate specificity and inhibitor studies of a membrane-bound ganglioside sialidase isolated from human brain tissue, Biol. Chem. 383 (2002) 1735–1742.
[22] T. Miyagi, T. Wada, K. Yamaguchi, K. Hata, Sialidase and malignancy: a minireview, Glycoconj. J. 20 (2004) 189–198.
[23] S. Proshin, K. Yamaguchi, T. Wada, T. Miyagi, Modulation of neuritogenesis by ganglioside-specific sialidase (Neu3) in human neuroblastoma NB-1 cells, Neurochem. Res. 27 (2002) 841–846.
[24] K. Yamaguchi, K. Hata, K. Koseki, K. Shiozaki, H. Akita, T. Wada, S. Moriya, T. Miyagi, Evidence for mitochondrial localization of a novel human sialidase (NEU4), Biochem. J. 390 (2005) 85–93.
[25] Y. Kakugawa, T. Wada, K. Yamaguchi, H. Yamanami, K. Ouchi, I. Sato, T. Miyagi, Up-regulation of plasma membrane-associated ganglioside sialidase (Neu3) in human colon cancer and its involvement in apoptosis suppression, Proc. Natl. Acad. Sci. U.S.A. 99 (2002) 10718–10723.
[26] P. Sun, X. Wang, K. Lopatka, S. Bangash, A.S. Paller, Ganglioside loss promotes survival primarily by activating integrin-linked kinase/Akt without phosphoinositide 3-OH kinase signaling, J. Invest. Dermatol. 119 (2002) 107–117.
[27] A. Sasaki, K. Hata, S. Suzuki, M. Sawada, T. Wada, K. Yamaguchi, M. Obinata, H. Tateno, H. Suzuki, T. Miyagi, Overexpression of plasma membrane-associated sialidase attenuates insulin signaling in transgenic mice, J. Biol. Chem. 278 (2003) 27896–27902.
[28] DS Modeling 1.1, Accelrys Inc., San Diego, CA, USA, 2003.
[29] A. Bairoch, R. Apweiler, The SWISS-PROT protein sequence database: its relevance to human molecular medical research, J. Mol. Med. 75 (1997) 312–316.
[30] S.F. Altschul, T.L. Madden, A.A. Schäffer, J. Zhang, Z. Zhang, W. Miller, D.J. Lipman, Gapped BLAST and PSI-BLAST: a new generation of protein database search programs, Nucl. Acids Res. 25 (1997) 3389–3402.
[31] H.M. Berman, J. Westbrook, Z. Feng, G. Gilliland, T.N. Bhat, H. Weissig, I.N. Shindyalov, P.E. Bourne, The protein data bank, Nucl. Acids Res. 28 (2000) 235–242.
[32] L.M. Chavas, C. Tringali, P. Fusi, B. Venerando, G. Tettamanti, R. Kato, E. Monti, S. Wakatsuki, Crystal structure of the human cytosolic sialidase Neu2: evidence for the dynamic nature of substrate recognition, J. Biol. Chem. 280 (2005) 469–475.
[33] J.D. Thompson, D.G. Higgins, T.J. Gibson, CLUSTAL W: improving the sensitivity of progressive multiple sequence alignment through sequence weighting, position-specific gap penalties and weight matrix choice, Nucl. Acids Res. 22 (1994) 4673–4680.
[34] A. Sali, T.L. Blundell, Comparative protein modeling by satisfaction of spatial restraints, J. Mol. Biol. 234 (1993) 779–815.
[35] R. Laskowski, M. MacArthur, D. Moss, J. Thornton, PROCHECK: a program to check the stereochemical quality of protein structures, J. Appl. Cryst. 26 (1993) 283–291.
[36] G. Vriend, A molecular modelling and drug design program, J. Mol. Graph. 8 (1990) 52–56.
[37] J. Pontius, J. Richelle, S.J. Wodak, Quality assessment of protein 3D structures using standard atomic volumes, J. Mol. Biol. 264 (1996) 121–136.
[38] R. Lüthy, J.U. Bowie, D. Eisenberg, Assessment of protein models with three-dimensional profiles, Nature 356 (1999) 83–85.
[39] W. Rocchia, S. Sridharan, A. Nicholls, E. Alexov, A. Chiabrera, B. Honig, Rapid grid-based construction of the molecular surface for both molecules and geometric objects: applications to the finite difference Poisson–Boltzmann method, J. Comp. Chem. 23 (2002) 128–137.
[40] M.L. Connolly, Solvent-accessible surfaces of proteins and nucleic acids, Science 221 (1983) 709–713.
[41] A. Hillisch, L.F. Pineda, R. Hilgenfeld, Utility of homology models in the drug discovery process, Drug Discov. Today 9 (2004) 659–669.
[42] D. Baker, A. Sali, Protein structure prediction and structural genomics, Science 294 (2001) 93–96.
[43] W. Kabsch, C. Sander, Dictionary of protein secondary structure: pattern recognition of hydrogen-bonded and geometrical features, Biopolymers 22 (1983) 2577–2637.
[44] G. Taylor, S. Crennell, C. Thompson, M. Chuenkova, Sialidases, in: B. Ernst, G.W. Hart, P. Sinaÿ (Eds.), Carbohydrates in Chemistry and Biology, 3, Wiley–VCH, Weinheim, 2000, pp. 485–495.
[45] V. Sobolev, A. Sorokine, J. Prilusky, E.E. Abola, M. Edelman, Automated analysis of interatomic contacts in proteins, Bioinformatics 15 (1999) 327–332.
[46] J.N. Watson, V. Dookhun, T.J. Borgford, A.J. Bennet, Mutagenesis of the conserved active-site tyrosine changes a retaining sialidase into an inverting sialidase, Biochemistry 42 (2003) 12682–12690.
[47] D.T.H. Chou, J.N. Watson, A.A. Scholte, T.J. Borgford, A.J. Bennet, Effect of neutral pyridine leaving groups on the mechanisms of influenza type A viral sialidase-catalyzed and spontaneous hydrolysis reactions of α-D-*N*-acetylneuraminides, J. Am. Chem. Soc. 122 (2000) 8357–8364.
[48] K.E. Lukong, K. Landry, M.A. Elsliger, Y. Chang, S. Lefrancois, C.R. Morales, A.V. Pshezhetsky, Mutations in sialidosis impair sialidase binding to the lysosomal multienzyme complex, J. Biol. Chem. 276 (2001) 17286–17290.
[49] Y. Wang, K. Yamaguchi, Y. Shimada, X. Zhao, T. Miyagi, Site-directed mutagenesis of human membrane-associated ganglioside sialidase: identification of amino-acid residues contributing to substrate specificity, Eur. J. Biochem. 268 (2001) 2201–2208.
[50] P. Politzer, P.R. Laurence, K. Jayasuriya, Molecular electrostatic potentials: an effective tool for the elucidation of biochemical phenomena, Environ. Health Perspect. 61 (1985) 191–202.
[51] N. Sinha, S.J. Smith-Gill, Electrostatics in protein binding and function, Curr. Protein Pept. Sci. 3 (2002) 601–614.
[52] P.K. Weiner, R. Langridge, J.M. Blaney, R. Schaefer, P.A. Kollman, Electrostatic potential molecular surfaces, Proc. Natl. Acad. Sci. U.S.A. 79 (1982) 3754–3758.
[53] Abstract No. P156, XVIII International Symposium on Glycoconjugates (GLYCO XVIII), Florence, Italy, September 4–9, 2005.